

Evaluating the impact of the weather conditions on the influenza propagation

David E. Singh

Universidad Carlos III de Madrid

Maria-cristina Marinescu (✉ mariacristina.marinescu@gmail.com)

Barcelona Supercomputing Center <https://orcid.org/0000-0002-6978-2974>

Jesus Carretero

Universidad Carlos III de Madrid

Concepcion Delgado-Sanz

Instituto de Salud Carlos III

Diana Gomez-Barroso

Instituto de Salud Carlos III

Amparo Larrauri

Instituto de Salud Carlos III

Research article

Keywords: influenza epidemic, simulation, meteorological model

Posted Date: September 4th, 2019

DOI: <https://doi.org/10.21203/rs.2.10422/v1>

License:   This work is licensed under a Creative Commons Attribution 4.0 International License.

[Read Full License](#)

Version of Record: A version of this preprint was published at BMC Infectious Diseases on April 5th, 2020.
See the published version at <https://doi.org/10.1186/s12879-020-04977-w>.

Evaluating the impact of the weather conditions on the influenza propagation

David E. Singh¹ and Maria-Cristina Marinescu² and Jesús Carretero¹ and Concepción Delgado-Sanz^{3,4} and Diana Gomez-Barroso^{3,4} and Amparo Larrauri^{3,4}

¹ Carlos III University of Madrid, Leganés, Spain

² Barcelona Supercomputing Center, Barcelona, Spain

³ CIBER en Epidemiología y Salud Pública (CIBERESP), Madrid, Spain

⁴ National Centre for Epidemiology, Carlos III Institute of Health, Madrid, Spain

Email: David E. Singh - dexposit@inf.uc3m.es; Maria-Cristina Marinescu* - mariacristina.marinescu@gmail.com; Jesús Carretero - jesus.carretero@uc3m.es; Concepción Delgado-Sanz - CDELGADOS@isciii.es; Diana Gomez-Barroso - DGOMEZ@externos.isciii.es; Amparo Larrauri - alarrauri@isciii.es;

*Corresponding author

Abstract

Background: Predicting the details of how an epidemic evolves is highly valuable as health institutions need to better plan towards limiting the infection propagation effects and optimizing their prediction and response capabilities. Simulation is a cost- and time-effective way of predicting the evolution of the infection as the joint influence of many different factors: interaction patterns, personal characteristics, travel patterns, meteorological conditions, previous vaccination, etc. The work presented in this paper extends EpiGraph, our influenza epidemic simulator, by introducing a meteorological model as a modular component that interacts with the rest of EpiGraph's modules to refine our previous simulation results. Our goal is to estimate the effects of changes in temperature and relative humidity on the patterns of epidemic influenza based on data provided by the Spanish Influenza Sentinel Surveillance System (SISSS) and the Spanish Meteorological Agency (AEMET).

Methods: Our meteorological model is based on the regression model developed by AB and JS, and it is tuned with influenza surveillance data obtained from SISSS. After pre-processing this data to clean it and reconstruct missing samples, we obtain new values for the reproduction number of each urban region in Spain, every 10 minutes during 2011. We simulate the propagation of the influenza by setting the date of the epidemic onset and the initial influenza-illness rates for each urban region.

18 Results: We show that the simulation results have the same propagation shape as the weekly influenza rates
19 as recorded by SISSS. We perform experiments for a realistic scenario based on actual meteorological data from
20 2010-2011, and for synthetic values assumed under simplified predicted climate change conditions. Results show
21 that a diminishing relative humidity of 10% produces an increment of about 1.6% in the final infection rate. The
22 effect of temperature changes on the infection spread is also noticeable, with a decrease of 1.1% per extra degree.

23 Conclusions: Using a tool like ours could help predict the shape of developing epidemics and its peaks, and
24 would permit to quickly run scenarios to determine the evolution of the epidemic under different conditions. We
25 make EpiGraph source code and epidemic data publicly available.

26 Keywords: influenza epidemic, simulation, meteorological model

27 **1 Background**

28 Seasonal influenza may not make headlines, but together with pneumonia, it is one of the top ten causes
29 of death worldwide. Influenza epidemics results in 3 to 5 million cases of severe illness a year, which puts
30 a high burden on health providers and results in loss of productivity and absenteeism, such as mentioned
31 by the World Health Organization in [1]. It's been long known that in temperate climates these seasonal
32 epidemics occur mostly in winter, and typical hypotheses assigned the blame to people being in closer
33 proximity for longer periods of time, or lowered immune systems. In general, meteorological conditions
34 affect virus transmission due to multiple effects: virus survival rates, host contact rates and immunity, and
35 the transmission environment (except the case of direct or short-range contact). While these factors may
36 have an influence, the solid evidence sustains the hypothesis that the virus's best surviving conditions are low
37 temperatures and low absolute humidity. One of the goals of the current research in this field is to understand
38 this relationship to be able to develop a more accurate seasonal influenza model for both temperate and
39 tropical regions. As a motivation of this work, JT et al. [2] conclude that environment factors may become
40 more important for a future predictive model of the effects of climate change. In a previous paper [3], some
41 of the authors of this paper studied the interaction of the spatio-temporal distribution of influenza in Spain
42 and the meteorological conditions during five consecutive influenza seasons. The work uses real influenza
43 and meteorological data in combination with statistical models to prove that there is a relationship between
44 the transmission of influenza and meteorological variables like absolute humidity and amount of rainfall. In
45 this work we use the same data sources (SISSS and AEMET agencies) following a different approach: we
46 study some of these relationships from a simulation perspective, considering not only the existing influenza

distributions but also the ones related to the climate change.

In this work we extend EpiGraph [4], an influenza simulator, with a meteorological model (MM) starting from the model developed by AB and JS [5]. In their paper AB and JS analyze monthly weather and influenza mortality data collected between 1973 and 2002 throughout all of the 359 US urban counties. Using a regression model, they conclude that there exist correlations between both absolute humidity and temperature with mortality. They report a quantitative assessment of the relation between mean daily humidity and temperature levels and mortality rates in different ranges. This is an extensive study and, as a result, we start from the assumption that their results are solid and appropriate to incorporate to EpiGraph in order to produce meteorological-dependent simulations based on real data. In this work we extend EpiGraph [4], an influenza simulator, with a meteorological model (MM) starting from the model developed by AB and JS [5]. In their paper AB and JS analyze monthly weather and influenza mortality data collected between 1973 and 2002 throughout all of the 359 US urban counties. Using a regression model, they conclude that there exist correlations between both absolute humidity and temperature with mortality. They report a quantitative assessment of the relation between mean daily humidity and temperature levels and mortality rates in different ranges. This is an extensive study and, as a result, we start from the assumption that their results are solid and appropriate to incorporate to EpiGraph in order to produce meteorological-dependent simulations based on real data.

Regarding other influenza simulators that consider weather conditions, PS et al. presents an agent-based simulation model [6] that evaluates the seasonal effects on the influenza propagation. Although the reproductive rates are generated synthetically without considering actual meteorological data, this paper shows, in a similar way than our work, the impact of changing reproductive rates on the course of the influenza pandemic. In the article [7], JS et al. simulate influenza transmission via a SIRS model modulated by climate data to obtain the basic reproduction number R_0 . Both JS et al. [8] and ACL et al. [9,10] study the effects of humidity on influenza transmission from the point of view of virus survival and conclude that aerosol transmission is most efficient in low humidity conditions. ACL et al. [9,10] and BX et al. [11] also conclude that aerosol transmission is more efficient at low temperatures. JS et al. [8] and JM et al. [12] also deduce that virus survival increases with decreasing the humidity values.

EpiGraph simulations use real data for modelling the population, the spatio-temporal distribution of influenza, and the meteorological conditions. This simulator consists of different components and data sources shown in Figure 1. The previous and novel components are represented in blue and orange colors, respectively. The simulator uses input data that is obtained from different sources including: (1) the influenza

78 data, that contains information about the initial individuals that are infected; (2) the population data, that
79 describes the individual interactions with others; (3) the transport data, that contains information about the
80 movement of individuals between different locations and (4) the climate data, that contains the meteorological
81 conditions existing during the simulated time span. This data feeds the different models implemented in the
82 simulator. We briefly describe the three models that have been previously developed and presented in [4,13].

83 The Epidemic model considers the propagation model of influenza extending the SIR (as explained in [14]
84 by FB et al.) to include states for latent, asymptomatic, dead and hospitalized. The infective period has
85 different phases which may affect the dissemination characteristics of the influenza virus as AME et al.
86 describe in [15]. Each individual has a slightly different length for each infection state. We adopt most of
87 the concrete values for the model parameters from the existing literature on flu epidemics (see [14–17]). You
88 can find them all in [18].

89 The transport component models the daily commute of individual to neighboring cities (inter-city move-
90 ment) and the long-distance travels for several days that represent commute of workers that need to reside
91 at different locations or people that move at any distance for vacation purposes. The people mobility model
92 is based on the gravity model proposed by CV et al. [19] that uses geographical information extracted from
93 Google using the Google Distance Matrix API service.

94 The social model is an agent model that captures individual characteristics and specifies the interaction
95 patterns based on existing interactions extracted from social networks. These patterns determine the close
96 contacts of each individual during the simulation, which is a crucial element to model the spread of the
97 infection. We extract interaction patterns from virtual interactions via email or social networks (Enron and
98 Facebook) and scale them to approximate a physical connection of the whole network within an urban area.
99 These connections are time-dependent to realistically capture the temporal nature of interactions, in our
100 case modeled depending on the day of the week and time of day. The distribution of the population is in
101 terms of four group types: school-age children and students, workers, stay-home parents, and retirees.

102 In this paper, as main contribution, we introduce a new component of the simulator (the meteorological
103 model), that evaluates the impact of climate parameters on influenza propagation. This component is tuned
104 with influenza surveillance data obtained from SISSS to provide realistic simulations. As far as we know, this
105 work is the first simulator that integrate real meteorological data to predict the spatio-temporal distribution
106 of influenza. We think that this contribution will help to better understanding the influenza propagation in
107 real environments.

108 In the literature we can find different influenza simulators although none of the following consider meteo-

109
110
111
112
113
114
115
116
117
118
119
120
121

rological factors in the simulation. Examples of them is the work of KK et al. [20] that presents an SIR-based epidemic simulator that permits to parametrize both the population characteristics and the epidemic process. The goal of this work is to identify the turning point (peak of the infected population) of the infection. Although the initial approaches for modelling the infection spreading across the contact network, our work consider a broader number of parameters and configuration of the network. HE et al. [21] analyze, by means of simulation, the relationship between social interaction patterns at workplaces and the virus transmission patterns during influenza pandemics. The main effort is geared towards the flexible specification of the different aspects involved in a simulation, such as intervention policies, social modelling, social organization of work, etc. SimFlu [22] is different from most epidemic simulators in that it focuses on the discovery of most probable future influenza variants starting from virus sequences published by the National Center for Biotechnology Information (NCBI). This work is complementary to the goal of most simulators, including ours, which is to understand and predict the spreading infection patterns of a known flu strand across a population. Their methodology is based on observing directional changes in subtypes of influenza over time.

122
123
124
125
126

JS and AK present a framework [23] to adjust an epidemic simulation based on real-time forecasts of infections from Google Flu Trends. The paper focuses on prediction of the timing of peak infection, but other metrics could be predicted as well. The authors of [24] simulate the spreading of influenza in an urban environment consisting of several close-by towns connected by trains. Their goal is to be able to model and simulate intervention policies.

127
128
129
130
131
132
133
134

Epiwork [25] was a European project in FP7 whose focus was to develop a tool framework for epidemic forecast. Within this project's framework, WB et al. describe GLEaMviz [26], their tool for epidemic exploration which includes a simulator of transmission based on an accurate demographics of world's population over which they superpose a (stochastic) mobility model. DB et al. [27] use human mobility extracted from airline flights and local commute (based on the gravity model) to predict the activity of the influenza virus based on Monte Carlo analysis. SM and SM [28] study the role of population heterogeneity and human mobility in the spread of pandemic influenza. In [29], the authors reconstruct contact and time-in-contact matrices from surveys and other socio-demographic data in Italy and use this matrix for simulation.

135 **2 Methods**

136 **2.1 Climate data pre-processing**

137
138

Epigraph uses meteorological data provided by the Spanish Meteorological Agency (AEMET) to generate environment-dependent influenza simulations. The pre-processing stage is performed to obtain clean inputs

139 for the meteorological model. First, the weather station nearest to each simulated urban region is identified.
140 Our simulations consider 92 different urban regions with more than 100,000 inhabitants. In some cases,
141 the station is within the city limits, while in others it is located in a nearby area (for instance at the
142 region’s airport). The data from each weather station is analyzed to reconstruct potentially missing samples.
143 Sometimes it is the case that some station data samples are missing because the station was not operational
144 during a given time period. These represents just a small fraction of the overall samples, but they have to be
145 properly addressed. Figure 2 shows an example of how the original missing data (shown in upper figure) is
146 reconstructed producing a complete sampling (reconstructed values are shown in the lower figure in red color).
147 In order to add the missing samples, we have used the reconstruct data algorithm (`missdata`) included in
148 the Matlab’s System Identification Toolbox. This toolbox permits the construction of mathematical models
149 for dynamic systems, starting from measured input-output data.

150 The resulting data is then processed to filter non-realistic values. Some weather stations produce abnor-
151 mal samples corresponding to non-realistic values that are too big or too small. Figure 2 shows an example
152 of this kind of values around sample 41,000. We have corrected these cases with a Matlab algorithm we
153 implemented to detect these peaks and correct them using an interpolation of the values from the previous
154 days. These two steps are only performed once for each new meteorological input data and the results may
155 be used for the rest of the process.

156 **2.2 Modeling the dependence of the infectious agent behavior on climate factors**

157 This section describes how the R_0 s are obtained from the meteorological conditions. In addition to the
158 notations introduced in the introduction, for the rest of the paper we will use SH for the specific humidity
159 and $P_{H_2O}^*$ for the equilibrium water vapor pressure.

160 In EpiGraph we adopt the results of the regression model used by AB and JS [5]. In their 2012 paper,
161 they analyze monthly weather and influenza mortality data collected between 1973 and 2002 throughout all
162 the 359 US urban counties. Using regression, they conclude that there exists a strong correlation between
163 absolute humidity and mortality, even when controlling for temperature, when the humidity drops below
164 daily means of 6g/kg. Temperature correlations also exist, mainly in the daily ranges between -1.1C and
165 15.6C. In an earlier paper ([7]) JS et al. study the same dataset and simulate influenza transmission
166 via a SIRS model modulated by the data to obtain the basic reproduction number R_0 . They also find
167 best-fit parameter range combinations of R_{0max} between 2.6 and 4, and R_{0min} between 1.05 and 1.3. We
168 adopt the pair of (R_{0max}, R_{0min}) that was found to be the best-fit parameter combinations they discover:

$R_{0max} = 3.52, R_{0min} = 1.12.$

From the definition of the specific humidity (SH) and relative humidity (RH)—see RHP and DWG [30]— we know that:

$$RH = SH * P / (0.622 + 0.378 * SH) * P_{H_2O}^* \quad (1)$$

We also know from Buck's equation that the equilibrium water vapor pressure can be calculated using the formula:

$$P_{H_2O}(T) = 0.61121 * Exp((18.678 - T/234.5)(T/(257.14 + T))) \quad (2)$$

where the temperature T is measured in degrees Celsius. This formula works best for values of T in the range of -80C to 50C. From known values RH , P , and T , and using equations (1) and (2), we can calculate the specific humidity.

From laboratory experiments by JS et al. [7] we have:

$$R_0 = exp(a * q + b) + R_{0min} \simeq exp(a * SH + b) + R_{0min} \quad (3)$$

where $a = -180$, $b = \log(R_{0max} - R_{0min})$ and q is the 2-m above-ground specific humidity, which we approximate to SH at the given temperature. In this way, we obtain a value for $P_{H_2O}^*$ in every sample (obtained every 10 minutes) using equation (2). From this value in combination with the values of RH and P we obtain the value of SH using equation (1). Finally, Equation (3) computes the new R_0 values for each urban region.

R_0 s are, therefore, time-dependent values that determine, in a stochastic process, how many susceptible individuals of an infected person's connections could be potentially infected. This is the dynamic component of the infectivity of an individual with respect to the others. The other dynamic component is the stochastic transition between infective states [4], computed with variable probabilities.

Our model is not different for the different types / subtypes of influenza. The values of the model parameters (basic reproduction numbers for each stage of the disease) were chosen to fall in the ranges published by AB and JS, which are based on actual data for all types of influenza, over 30 years. We choose fixed R_0 s within the ranges, although this is a parameter that can be configured to vary. On the other hand, the evaluation was performed over data from the 2010-2011 influenza season over the whole territory of Spain, for all types of influenzas that were diagnosed. We consider that both the choice of R_0 (based on

196 exhaustive data) and the evaluation against real reported cases across Spain are comprehensive enough to
197 validate our results.

198 **2.3 Simulator setup**

199 *2.3.1 Setting up the influenza model*

200 The Spanish Influenza Sentinel Surveillance System (SISSS) comprises 17 networks of sentinel physicians
201 (general practitioners and pediatricians) in 17 of the 19 Spanish regions, as well as the network-affiliated
202 laboratories, including the National Influenza Reference Laboratory (National Centre for Microbiology, World
203 Health Organization National Influenza Centre in Madrid). More than 800 sentinel physicians participated
204 each season covering a population under surveillance of around one million—see [31,32]. Sentinel physicians
205 reported influenza-like illness (ILI) cases—integrating virological data collected in the same population—
206 detected in their reference populations on a weekly basis, following a definition based on the EU-ILI, as
207 described in [33]. For influenza surveillance, they systematically swab (nasal or nasopharyngeal) the first
208 two ILI patients each week and sent the swabs to the network-affiliated laboratories for influenza virus
209 detection. The information collected by the SISSS includes data on demographics, clinical and virological
210 characteristics, seasonal vaccination status, chronic conditions, and pregnancy. Data is entered weekly by
211 each regional sentinel network in a web-based application [34] and analyzed by the National Centre of
212 Epidemiology to provide timely information on the evolving influenza activity in Spanish regions and at
213 the national level. For example, during the 2011-2012 season, 651 sentinel physicians and 236 pediatricians
214 participated to SISSS and surveyed a total population of 1,142,189, which represents 2.36% of the total
215 population of Spain.

216 We obtained the SISSS data from the National Center of Epidemiology, Institute of Health Carlos III of
217 Madrid (ISCIII). In order to produce realistic simulations, EpiGraph has to be properly configured. This
218 configuration process consists of setting up two parameters: the date of the epidemic onset and the initial
219 influenza-illness rates for each urban region.

220 The first parameter is the time of onset of the epidemics, which occurs during week 50 of 2010. At this
221 time the national average incidence values for influenza are greater than 60 cases per 100,000 inhabitants,
222 which is the threshold determined by SISS, based on data from the 2010-2011 seasonal epidemic, to be the
223 start of the influenza season. In our simulation the exact date is the 13th of December of 2010.

224 The second parameter values were obtained from influenza surveillance data obtained from the SISSS

corresponding to the influenza season 2010-11. From this data we obtained the reported weekly ILI rate at national and regional level in Spain. The data for the Murcia and Galicia communities are not available and we approximated them based on the data from the nearest community. These rates allow us to approximate the initial number of (clinically) influenza-like-infected individuals using the following formula, based on the study published online (in March 2017) in the Lancet Respiratory Medicine by ACH et al. [35].

$$N_{tot} = \frac{N_{report}}{Symp * Attend} * F_{pos}, \quad (4)$$

where N_{report} are the cases that demanded medical attention, as reported by the SSISS, F_{pos} is the fraction of positive cases, $Symp$ is the percentage of symptomatic individuals, and $Attend$ is the percentage of those with symptoms that see a doctor. For instance, for the reported $N_{report} = 90$ cases per 100,000 inhabitants in week 50, and with values $F_{pos} = 33\%$ (empirical value for 2010-2011 in Spain), and $Symp = 23\%$, $Attend = 17\%$ (values taken from the cited study), we calculate that the total number of infected individuals is of approximately 765 cases per 100,000 inhabitants - or 0.765% of the total population. We use this value to set up the initial conditions of the simulation (described in this section), but also to validate its results. Each community has a different N_{report} , which leads to different numbers of initially infected individuals.

EpiGraph allows modeling at the level of each individual, and thus can simulate the effect of vaccination policies. To produce realistic results, we use different influenza vaccination coverages by age group; for those older than 65 we have used the vaccination ratios (per community) provided by the Ministry of Health, Social Services, and Equality of Spain. These values correspond to vaccination coverages collected by the National Health System [36]. For the rest of the population (individuals younger than 65) we have used the data provided by the Spanish Statistical Office, which is based on surveys done in each community. Given that the data are available at community level, we assume that all the urban areas located in the same community have the same vaccination coverages. Table 1 shows these percentages per community and age.

As input of the mobility model, we use 85% workers and 15% students for short distance travel, and 50% workers, 30% students, 15% retired individuals, and 5% unemployed for long distance travel.

2.3.2 Calibrating the simulator

While EpiGraph accounts for many of the components that influence the spreading of the virus, the behavior of these parts and the values of the parameters (such as the initial infectious individuals or the vaccination rate) are unavoidably approximate. On their website, the World Health Organization reports that in annual

254 influenza epidemics, 5-15% of the population are affected with upper respiratory tract infections [1]. We
255 have therefore introduced a scaling factor which adjusts the infection propagation rate of each individual to
256 produce, for each urban region, a final infection rate between 10% and 14% of the total population. These
257 values are obtained in a pre-calibration phase of EpiGraph for the real climate conditions—performed only
258 once— and are then used for all subsequent simulation experiments. Note that we are using data from
259 SSISS, which records influenza-like-illness cases that are not confirmed by laboratory tests. This fact doesn't
260 affect the validity of our results because the purpose is to compare yearly/monthly numbers under different
261 climate conditions rather than know the accurate number of infected individuals.

262 **2.4 Experimental setup**

263 We have performed different tests to validate our approach and simulator. We first validated the simulator
264 against influenza surveillance data, then we evaluated two different environmental scenarios. We believe
265 that our simulator can be useful to predict the short- and medium-term spread of an infection, as well as to
266 assess the effects that changes in climate can have over influenza epidemics worldwide.

267 The first scenario involves real climate values from AEMET and allows studying the short- and medium-
268 term propagation for influenza strands. For the second set of scenarios we generate fictitious values of
269 RH and T by scaling the real values. Our idea is to study the effects of the changing climate conditions on
270 influenza propagation. Simulations occur across the 92 largest cities in Spain, which account for a population
271 of 21,320,965 inhabitants. The time span is 7 months starting from the day identified as the onset date in
272 our data - the 13th of December of 2010.

273 In our experiments we have used data from 92 weather stations from the national network, distributed
274 across the country. Each weather station collects the values of temperature, atmospheric pressure, and
275 relative humidity every 10 minutes during the entire 2011. These consists of about 157,000 data samples
276 per station and 14.5 million data values in total. Based on these values, we generate the basic reproduction
277 numbers to obtain an R_0 value per urban area at every 10 minutes. With the previously determined initial
278 influenza-like rates per region and (year-specific) date of onset, and after calibration, each urban region data
279 - vaccination rates, individuals' characteristics, initial infective individuals, and R_0 s values - are loaded from
280 files.

3 Results

3.1 Validation of the simulator quality

The validation of our simulator in terms of its capacity to predict qualitatively similar propagation results as those approximated from the influenza surveillance data recorded by SSISS. The simulated values for each of the Spanish regions are the aggregated values of all the urban regions belonging to it.

Figure 3 shows the simulated and actual estimated data. The simulated values are scaled to make the largest simulated value to be the same as the maximum real value. This allows a comparison of the evolution of the influenza propagation for each community over time. We can observe that we obtain a prediction similar in shape to the real values for each region.

The reason for scaling the data is that that the simulated and actual estimated data reflect the population rather differently. On one hand, the simulated values correspond to the overall number of individuals infected with influenza across the considered urban areas. These take into account all the individuals within the simulated areas but only include the largest urban regions (above 100,000 inhabitants); small cities, towns, and villages are not considered. On the other hand, the influenza surveillance data are only related to a small fraction of the existing clinical cases: SSISS covers a representative but small percentage of the population, in addition to the fact that there are more cases than those reported due to people not seeking medical attention. In contrast, the number of cases are collected from the complete community (including both large and small populations). It is thus not possible to compare the absolute values of the two data sources, although they should be linearly related.

3.2 Effect of long-term climate changes

Figure 4 shows an example of the value of these parameters for the urban region of Terrasa (Barcelona) over one year. We can observe strong variations of R_0 that are related to the changing temperature, relative humidity, and pressure conditions.

To evaluate the effect of both real and hypothetical meteorological climate changes on the spreading of influenza we evaluate temperature variations of ΔT degrees and percentage variations of the relative humidity pRH . $\Delta T = 0$ and $pRH = 1.0$ correspond to the initial scenario with the original climate conditions. Studies show that climate change is producing increments in the average temperature (amplified by pollution) and, in southern Europe, longer periods of drought. The idea is to evaluate the impact of these changes on the influenza propagation. In this section, we consider long-term meteorological climate changes, that is, changes in the climate conditions that extend to the entire simulated period of 28 weeks. In this context, we evaluate

311 two different scenarios, probably not as complex as future real climate changes.

312 The first one corresponds to drought conditions, when the relative humidity values (RH) are smaller than
313 current ones. We have considered a reduction of the relative humidity from 90% to 50% in increments of
314 10% (RH values half than the original ones). According to the infection model, influenza propagates easier
315 for smaller RH values; we thus expect to observe a larger effect. Figure 5 shows the overall percentage of
316 infected individuals per community predicted by EpiGraph. The diminishing RH has indeed a strong impact
317 on the number of infected individuals. On average, 12.4% of the population was infected in the base case
318 (reduction factor equal to 1), while the average infection rate for 0.5 factor is 20.5%. We can observe that a
319 percental reduction of RH of 10% produces an approximate increment of 1.6% in the final infection rate.

320 The second scenario evaluates the impact of an increase of temperature on the propagation. Figure 6
321 shows the final infection rate for an increment of the temperature between 0 degrees (current case) and 5
322 degrees Celsius. We can observe that now there is a reduction in the infection rate when the temperature
323 increases. Now, an increment of 5 degrees reduces the average infection rate from 12.5% to 6.9%—a decrement
324 of 1.1% per degree.

325 Both scenarios assume that the values of the parameters (RH, T) change one at a time. This is a
326 simplification, and the idea behind this approach is to evaluate the impact of a single parameter variation on
327 the overall influenza outcome. However, EpiGraph supports specifying any changing combination of climate
328 conditions. In a more realistic scenario both parameters would change, and the climate specialists are those
329 who should define what the concrete values are.

330 Figure 7 shows the combined effect of temperature and relative humidity change on the average nation-
331 wide infection rate. We have plotted two planes: the first one (colored) represents the average infection
332 rates for different increments in the temperature values and percentile reductions in the relative humidity;
333 the second one (green) displays the infection rate of the original scenario (without climate variation) for all
334 the coordinates and represents the baseline case. The two planes intersect in the lower-left point, where the
335 temperature and RH have the original values. Although both parameters influence the final infection rate,
336 relative humidity has a larger effect than temperature.

337 Figure 8 shows the effect of RH and temperature variations on the infection distribution for Andalusia
338 community. We can observe that the variation of both parameters changes the shape of the distribution,
339 especially in terms of the peak values but also - more subtly - in terms of the propagation interval.

340 The maximum and minimum 95% confidence intervals baseline scenario (no RH reduction nor tempera-
341 ture increment) ranges between 0.28 and 0.06 for urban areas in Castilla la Mancha and Aragón, respectively.

These results are produced by a simulator repeating the simulations 30 times. Note that there already exist 342
uncertainty in the input data, both with respect to the number of initially infected individuals as well as 343
from the point of view of the epidemic model. 344

3.3 Effect of short-term climate changes 345

To evaluate the effect of short-term changes in climate conditions, we modify RH and the temperature 346
exactly like described in the previous section, only for the first week of the simulation. The rest of the 347
simulation uses the original climate parameters. Figures 9 and 10 show the final infection rate for different 348
variations of RH and temperature. We can observe that the impact on the overall percentage of infected 349
individuals is still important, particularly for a decrease in RH of 0.2 or more and - less evidently - for an 350
increase in temperature of 3 degrees or more. For smaller changes in temperature the effect is less evident, 351
but we believe that this is due to the fact that the short-term simulation of temperature increase is only one 352
week. 353

4 Discussion 354

We achieve herd immunity in two ways: as result of vaccinating campaigns, and naturally when an individual 355
that was infected goes to the recovery (or dead) state, in which case he becomes immune and starts acting 356
as a propagation stopper. As a result, after certain threshold of infected vs susceptible individuals, the 357
infection rate naturally goes down. This occurs at the inflection point in the propagation graph, specifically 358
at about 16 weeks (in our data). The vaccination success rate during the 2010-2011 season was approximately 359
50% [37]. Given the parameters shown in Fig. 4 of [38] for herd immunity for influenza, we consider that 360
the R_0 considered by our model takes into consideration this type of immunity. We do not model the level 361
at which herd immunity starts acting as a parameter, although this phenomenon occurs naturally in the 362
simulations. The simulator is flexible enough to support different daily contact patterns for each individual. 363
The probability of an individual getting infected during an interaction also differs (it's a stochastic process), 364
and thus the infection can be transmitted to individuals pertaining to different groups. 365

A possible limitation is that we only model the largest 92 urban regions in Spain; we could add more 366
information related to smaller cities and towns, including rural regions. Nevertheless we don't think this 367
data would make a significant difference in the results, as the infection needs a large number of hosts to 368
explode, and / or travel patterns between the infected areas. Small town and village areas are arguably 369
much less likely than cities to fulfill these roles. 370

371 A second limitation is related to the meteorological factors affecting the infection propagation: the
372 number and set of climate factors that the meteorological model takes into account, and the choice of the
373 model itself. Additional parameters that specialists mention as possible influencers in virus transmission are
374 factors such as wind, precipitation, or pollution.

375 One important thing to underline is that the data that the study [5] (whose model we adopt) is based
376 on is of real cases and spans 30 years. Interactions between meteorological trends and human behavior are
377 therefore intrinsically reflected in the data, although the rules of behavior change are not explicitly specified
378 for the agents (i.e. individuals) involved in the simulation. The case can be made that meteorological changes
379 were not as extreme before 2002, and that a regression model based on new data may change as well over
380 time. While this is a definite possibility, we believe that its nature will not change in a fundamental way,
381 such that we can still predict trends, if not absolute values.

382 Finally, to successfully simulate the flu epidemics requires leveraging many different types of data, most
383 of them in large amounts, as input and calibration measurements for our tool (EpiGraph). For instance,
384 we are using social network data from Enron and Facebook to set up the population interaction patterns,
385 census data to extract the characteristics of the different types of individuals, Google Maps to initialize
386 the transportation module, data from AEMET to run simulations that are realistic from a meteorological
387 viewpoint, and weekly ILI rates obtained from the SISSS to initialize and evaluate the simulator. This makes
388 the implementation of EpiGraph more realistic, a strength that can lead to more accurate simulations.

389 **5 Conclusions**

390 We have extended our simulator EpiGraph with a meteorological model that interacts with the rest of the
391 system to better reflect the behavior of the influenza propagation through the entire population of Spain. To
392 produce realistic results we also take into account vaccination, with different ratios based on the individuals'
393 ages. The simulator results are compared to real data on infection rates and across the whole country.
394 The results for the prediction of the evolution of the influenza propagation for each community over time
395 are similar in shape to the real data. After validating the simulator, we evaluate different scenarios that
396 reflect changes in climate conditions, and show the predictions for variations in the relative humidity and
397 temperature. Lastly, we make EpiGraph's source code publicly available at [18], to be used by the scientific
398 community.

399 As future work, an interesting, although independent, possibility is to investigate the potential of Epi-
400 Graph to simulate the evolution of the virus spread for different subtypes of influenza, once the propagation

model parameters (e.g. incubating period, infectious period, basic reproduction numbers, etc.) are known, 401
or to narrow down the possible subtypes in early phases of an infection. One could also investigate the 402
impact of new meteorological factors on the evolution of the infection. 403

List of abbreviations 404

SISSS: Influenza Sentinel Surveillance System 405

AEMET: Spanish Meteorological Agency 406

MM: EpiGraph’s meteorological model 407

SIR/SIRS: Susceptible Infected Recovered / - Susceptible 408

SH: specific humidity 409

RH: relative humidity 410

T: temperature 411

P: atmospheric pressure 412

ILI: influenza-like illness 413

ISCIH: Institute of Health Carlos III of Madrid 414

6 Declarations 415

Ethics approval and consent to participate Not applicable. 416

Consent for publication Not applicable. 417

Availability of data and material 418

EpiGraph’s User Manual and source code are publicly available at [18] and can be used by the scientific 419
community. The dataset supporting the conclusions of this article is available in the [39] repository. 420

Competing interests The authors declare that they have no competing interests. 421

Funding This work has been partially supported by the Spanish ”Ministerio de Economía y Competi- 422
tividad” under the project grant TIN2016-79637-P ”Towards Unification of HPC and Big Data paradigms”. 423
The work of Maria-Cristina Marinescu has been partially supported by the Spanish “Ministerio de Economía 424
y Competitividad” under project grant SEMIOTIC (ref. TIN2016-78473-C3-2-R). The role of both funders 425
was limited to financial support and did not imply participation of any kind in the study and collection, 426
analysis, and interpretation of data, nor in the writing of the manuscript. 427

Authors’ contributions 428

429 David E. Singh, Maria-Cristina Marinescu and Jesús Carretero designed and implemented EpiGraph
430 simulator. All authors conceived and designed the experiments. David E. Singh processed the input data
431 and run the experiments. David E. Singh and Maria-Cristina Marinescu wrote the paper. All authors review
432 the different manuscript drafts and approved the final version for submission.

433 Acknowledgments

434 We would like to acknowledge all the sentinel general practitioners and pediatricians, epidemiologists,
435 and virologists participating in the Spanish Influenza Sentinel Surveillance System. Part of the input data
436 used in this work have been obtained from the Spanish Influenza Sentinel Surveillance System and the
437 meteorological information provided by Spanish National Meteorological Agency, AEMET, Ministerio de
438 Agricultura, Alimentación y Medio Ambiente.

439 References

- 440 1. World Health Organization *Influenza (Seasonal). Fact sheet NOV 2016.*
441 <http://www.who.int/mediacentre/factsheets/fs211> 2016.
- 442 2. Tamerius J, Nelson M, Zhou S, Viboud C, Miller M, Alonso W: **Global influenza seasonality: reconciling**
443 **patterns across temperate and tropical regions.** *Environmental Health Perspective* 2010, **119**(4):439–445.
- 444 3. Gomez-Barroso D, León-Gómez I, Delgado-Sanz C, Larrauri A: **Climatic Factors and Influenza Transmis-**
445 **sion, Spain, 2010–2015.** *International Journal of Environmental Research and Public Health* 2017, **14**(12),
446 [<http://www.mdpi.com/1660-4601/14/12/1469>].
- 447 4. Martin G, Marinescu MC, Singh D, Carretero J: **Leveraging social networks for understanding the evo-**
448 **lution of epidemics.** *BMC System Biology* 2011, **5**(S3).
- 449 5. Barreca A, Shimshack J: **Absolute Humidity, Temperature, and Influenza Mortality: 30 Years of**
450 **County-Level Evidence from the United States.** *American Journal of Epidemiology* 2012, **176**(7).
- 451 6. Shi P, Keskinocak P, Swann JL, Lee BY: **Modelling seasonality and viral mutation to predict the course**
452 **of an influenza pandemic.** *Epidemiology and Infection* 2010, **138**(10):1472–1481.
- 453 7. Shaman J, Pitzer V, Viboud C, Grenfell B, Lipsitch M: **Absolute Humidity and the Seasonal Onset of**
454 **Influenza in the Continental United States.** *Plos Biology* 2010, **8**(2).
- 455 8. Shaman J, Kohn M: **Absolute humidity modules influenza survival, transmission, and seasonality.**
456 *Proc. National Academy of Science, USA* 2009, **106**:3243–3248.
- 457 9. Lowen A, Mubareka S, Palese P: **Influenza virus transmission is dependent on relative humidity and**
458 **temperature.** *PLoS Pathology* 2007, **3**:1470–1476.
- 459 10. Lowen A, Mubareka S, Palese P: **High temperatures (30 degrees C) blocks aerosol but not contact**
460 **transmission of influenza virus.** *Journal of Virology* 2008, **82**:5650–5652.
- 461 11. Xu B, Jin Z, Jiang Z, Guo J, Timberlake M, Ma X: **Climatological and geographical impacts on global**
462 **pandemic of influenza A(H1N1).** *Global urban monitoring and assessment through Earth observation* 2014.
- 463 12. McDevitt J, Rudnick S, First M, Spengler J: **Role of absolute humidity in the inactivation of influenza**
464 **viruses on stainless steel surfaces at elevated temperatures.** *Applications Environmental Microbiology*
465 2010, **76**(12):3943–3947.
- 466 13. Martin G, Singh D, Marinescu MC, Carretero J: **Towards efficient large scale epidemiological simulations**
467 **in EpiGraph.** *PARCO* 2015, **42**:88–102.
- 468 14. Brauer F, Driessche Pvd, Wu J (Eds): *Mathematical Epidemiology.* Springer, 1 edition 2008.

15. Alexander ME, Bowman CS, Feng Z, Gardam M, Moghadas SM, Roest G, Wu J, Yan P: **Emergence of drug resistance: implications for antiviral control of pandemic influenza.** *Proceedings of the Royal Society* 2007, **274**:1675–1684. 469
470
471
16. Longini IM, Halloran EM, Nizam A, Yang Y: **Containing Pandemic Influenza with Antiviral Agents.** *Am. J. Epidemiol.* 2004, **159**(7):623–633. 472
473
17. Elveback LR, Fox JP, Ackerman E, Langworthy A, Boyd M, Gatewood L: **An influenza simulation model for immunization studies.** *American Journal of Epidemiology* 1976, **103**(2):152–165. 474
475
18. *Computer Architecture Group. University Carlos III of Madrid. Epigraph source code and User Manual.* git-lab.arcos.inf.uc3m.es:8380/desingh/EpiGraph. 476
477
19. Viboud C, Bjørnstad ON, Smith DL, Simonsen L, Miller MA, Grenfell BT: **Synchrony, waves, and spatial hierarchies in the spread of influenza.** *Science* 2006, **312**:447–451. 478
479
20. Kim K, Lee S, Lee D, Lee KH: **Coupling effects on turning points of infectious diseases epidemics in scale-free networks.** *BMC Bioinformatics* 2017, **18**(7):79–88. 480
481
21. Timpka T, Eriksson H, Holm E, Strömberg M, Ekberg J, Spreco A, Dahlström: **Relevance of workplace social mixing during influenza pandemics: an experimental modelling study of workplace cultures.** *Epidemiology and Infection* 2016, **144**(10):2031–2042. 482
483
484
22. Ahn I, Kim HY, Jung S, Lee JH, Son HS: **SimFlu: a simulation tool for predicting the variation pattern of influenza A virus.** *Computers in biology and medicine* 2014, **52**:35–40. 485
486
23. Shamana J, Karspeckb A: **Forecasting seasonal outbreaks of influenza.** *Proceedings of the national academy of sciences of the USA* 2012, **109**(50):20425–20430. 487
488
24. Saito M, Imoto S, Yamaguchi R, Miyano S, Higuchi T: **Parallel agent-based simulator for influenza pandemic.** In *AAMAS 2011 Workshops, Volume 361-370* 2011. 489
490
25. *European Commission. Framework programme 7-ICT. (CORDIS) EPIWORK.* <http://epiwork.eu/> 2009. 491
26. den Broeck WV, Gioannini C, Gonçalves B, Quaggiotto M, Colizza V, Vespignani A: **The GLEaMviz computational tool, a publicly available software to explore realistic epidemic spreading scenarios at the global scale.** *PubMed BMC Infectious Disease* 2011, **11**(37). 492
493
494
27. Balcan D, Hu H, Goncalves B, Bajardi P, Poletto C, Ramasco JJ, Paolotti D, Perra N, Tizzoni M, den Broeck WV, Colizza V, Vespignani A: **Seasonal transmission potential and activity peaks of the new influenza A(H1N1): a Monte Carlo likelihood analysis based on human mobility.** *BMC Medicine* 2009, **7**(45). 495
496
497
28. Merler S, Ajelli M: **The role of population heterogeneity and human mobility in the spread of pandemic influenza.** *Proc Biol Sci* 2010, **277**(1681). 498
499
29. Iozzi F, Trusiano F, Chinazzi M, Billari F, Zagheni E, Merler S, Ajelli M, Fava ED, Manfredi P: **Little Italy: An Agent-Based Approach to the Estimation of Contact Patterns- Fitting Predicted Matrices to Serological Data.** *Plos Computational Biology* 2010. 500
501
502
30. Perry R, Green D: *Perry's Chemical Engineers' Handbook (7th Edition).* McGraw-Hill 2007. 503
31. Larrauri A dMS: **Characterisation of swabbing for virological analysis in the Spanish Influenza Sentinel Surveillance System during four influenza seasons in the period 2002-2006.** *Euro Surveill* 2007, **12**(5:E5-E6). 504
505
506
32. Larrauri C, Jimenez-Jorge S, de Mateo S, Pozo S, Ledesma M, Casas F: **Epidemiology of the 2009 influenza pandemic in Spain. The Spanish Influenza Surveillance System.** *Enferm Infecc Microbiol Clin* 2012, **30**(S4:2-9). 507
508
509
33. European Commission: *Commission Decision of 30 April 2009 amending Decision 2002/253/EC laying down case definitions for reporting communicable diseases to the Community network under Decision No 2119/98/EC of the European Parliament and of the Council.* Luxembourg: Publications Office of the European Union. 2009. 510
511
512
34. *Instituto de Salud Carlos III. Regional Sentinel Network.* <http://vgripe.isciii.es/gripe>. 513
35. Hayward AC, et al.: **Comparative community burden and severity of seasonal and pandemic influenza: results of the Flu Watch cohort study.** *Lancet Respiratory Medicine* 2014, **2**: 445–54. 514
515

- 516 36. *Ministerio de Sanidad, Servicios Sociales e Igualdad. Coberturas de vacunación en mayores de 65*
517 *años. Temporada estacional 2011-2012.* [http://www.msssi.gob.es/ciudadanos/enfLesiones](http://www.msssi.gob.es/ciudadanos/enfLesiones/enfTransmisi-)
518 [/enfTransmisi-](http://www.msssi.gob.es/ciudadanos/enfTransmisi-)
[bles/gripe/coberturas.htm](http://www.msssi.gob.es/ciudadanos/enfTransmisi-).
- 519 37. Jiménez-Jorge S, Savulescu C, Pozo F, de Mateo S, Casas I, Ledesma J, Larrauri A: **Effectiveness of the**
520 **2010–11 seasonal trivalent influenza vaccine in Spain: cycEVA study.** *Vaccine* 2012, **30**(24):3595 –
521 3602, [<http://www.sciencedirect.com/science/article/pii/S0264410X12004409>].
- 522 38. Plans-Rubió P: **The vaccination coverage required to establish herd immunity against in-**
523 **fluenza viruses.** *Preventive Medicine* 2012, **55**:72 – 77, [[http://www.sciencedirect.com/science/article/pii/](http://www.sciencedirect.com/science/article/pii/S0091743512000588)
524 [S0091743512000588](http://www.sciencedirect.com/science/article/pii/S0091743512000588)].
- 525 39. *Computer Architecture Group. University Carlos III of Madrid. EpiGraph 1.3 meteorological-based experimental*
526 *data.* <http://doi.org/10.5281/zenodo.836515> 2017.

Table 1: Proportion of influenza vaccinated population by Spanish region.

Age group	Andalucía	Aragón	Asturias	Balears	Cantabria	Castilla y León
16-64 years	21.8	20.4	23.8	18.0	22.5	27.7
>64 years	60.0	57.5	56.2	45.9	57.3	66.1
	C. Valenciana	Extremadura	Galicia	C. de Madrid	Murcia	Navarra
16-64 years	20.9	24.4	22.9	23.6	24.0	22.5
>64 years	50.6	50.8	52.4	58.2	49.3	60.1
	Castilla la Mancha	Cataluña	País Vasco	Rioja		
16-64 years	23.4	21.7	24.2	21.4		
>64 years	54.0	54.0	60.3	66.5		

Figure 1: Overview of the data sources, processed data, and EpiGraph components.

Figure 2: Data reconstruction example of temperature values for Alcobendas urban region (the reconstructed values are in red color). X-axis units corresponds to tens of thousand samples and the total number of samples displayed is 52,560 (one sample every 10 minutes for one-year span).

Figure 3: Comparison of normalized values between EpiGraph (in red) and real values (in blue) for Navarra, Madridm País Vasco and Valencia communities. Real values correspond to the total number of infected N_{tot} , obtained by means Equation 4 from influenza surveillance data.

Figure 4: Meteorological parameters (T, RH, P) and the obtained R0s values for a one-year simulation (2011) for Tarrasa urban area.

Figure 5: Effect of long-term changes of relative humidity on the influenza propagation for the different communities considered in the simulation.

Figure 6: Effect of long-term changes in the temperature on the influenza propagation for the different communities considered in the simulation.

Figure 7: Effect of long-term changes in the relative humidity (percentil reduction) and temperature (value increment in Celsius) on the influenza propagation for the average nation-wide infection rates.

Figure 8: Effect of long-term parameter variation on the infection distribution shape for Andalucía. In (a) different RH scales are evaluated (100% in red, 90% in green, 80% in blue and 70% in black); In (b) different temperature offsets are evaluated (0 degrees in red, +1 degrees in green, +2 degrees in blue and +3 degrees in black).

Figure 9: Effect of short-term changes in the relative humidity on the influenza propagation for the different communities considered in the simulation.

Figure 10: Effect of short-term changes in the temperature on the influenza propagation for the different communities considered in the simulation.

Figures

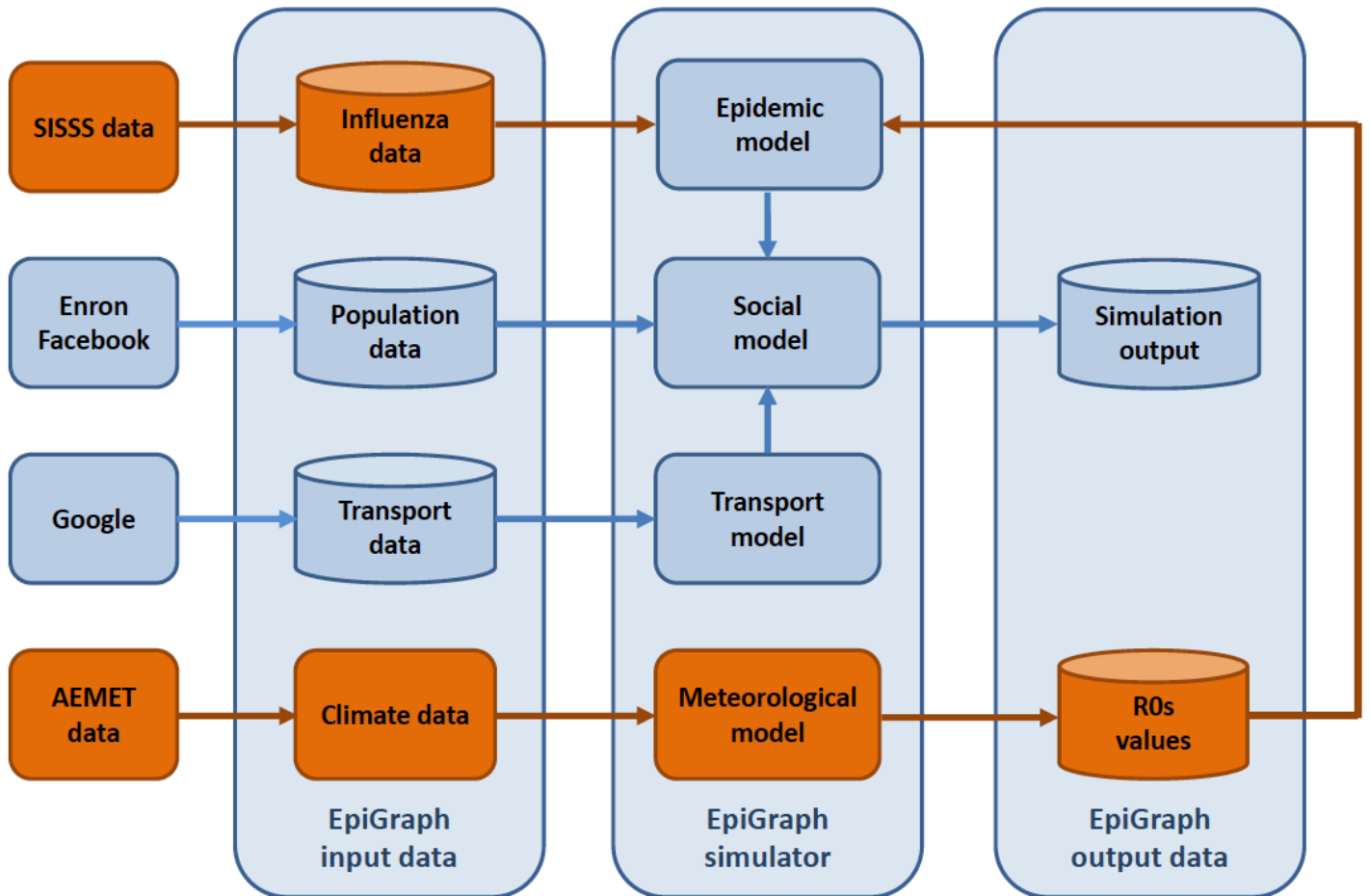


Figure 1

Overview of the data sources, processed data, and EpiGraph components.

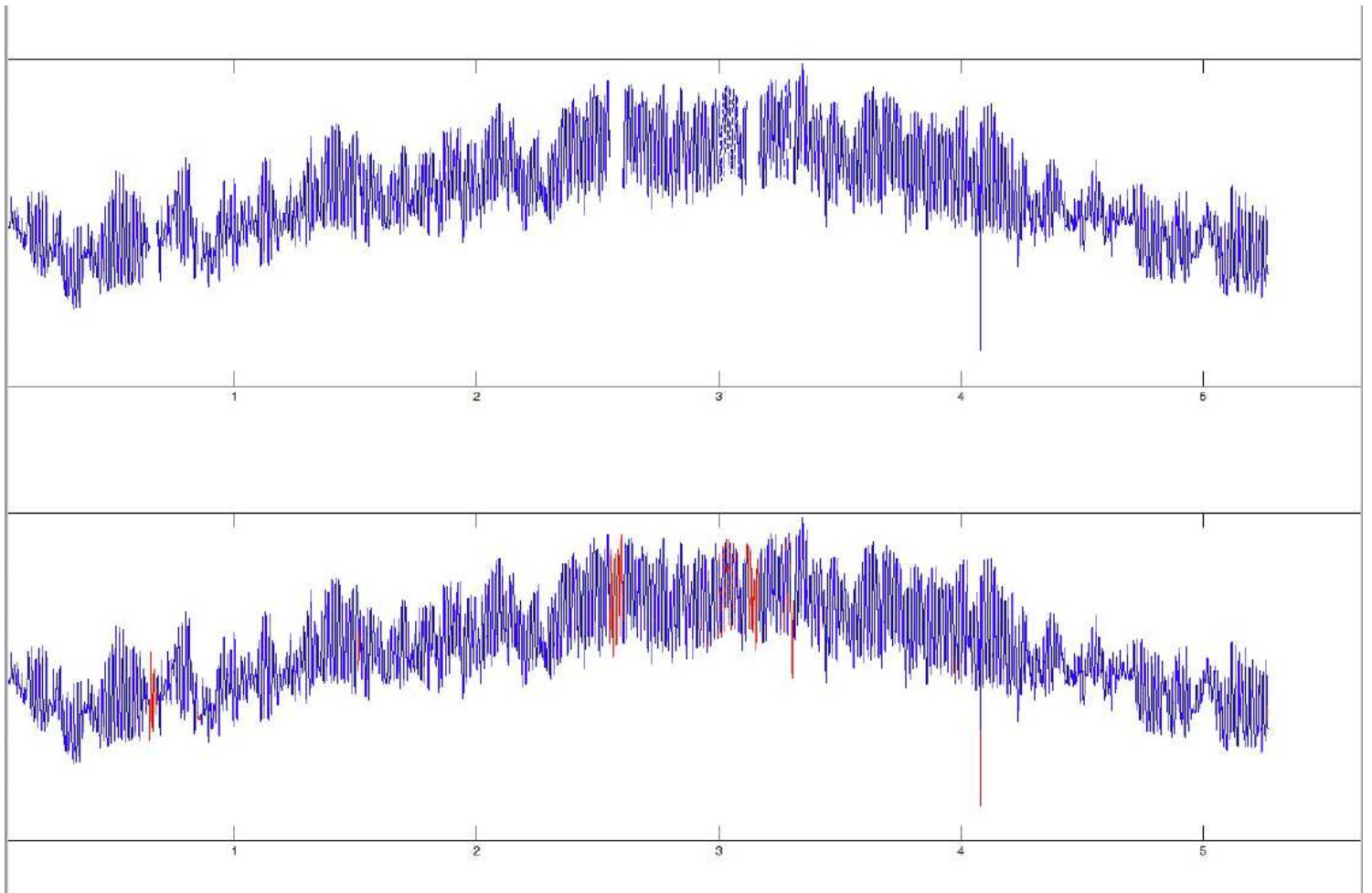


Figure 2

Data reconstruction example of temperature values for Alcobendas urban region (the reconstructed values are in red color). X-axis units corresponds to tens of thousand samples and the total number of samples displayed is 52,560 (one sample every 10 minutes for one-year span).

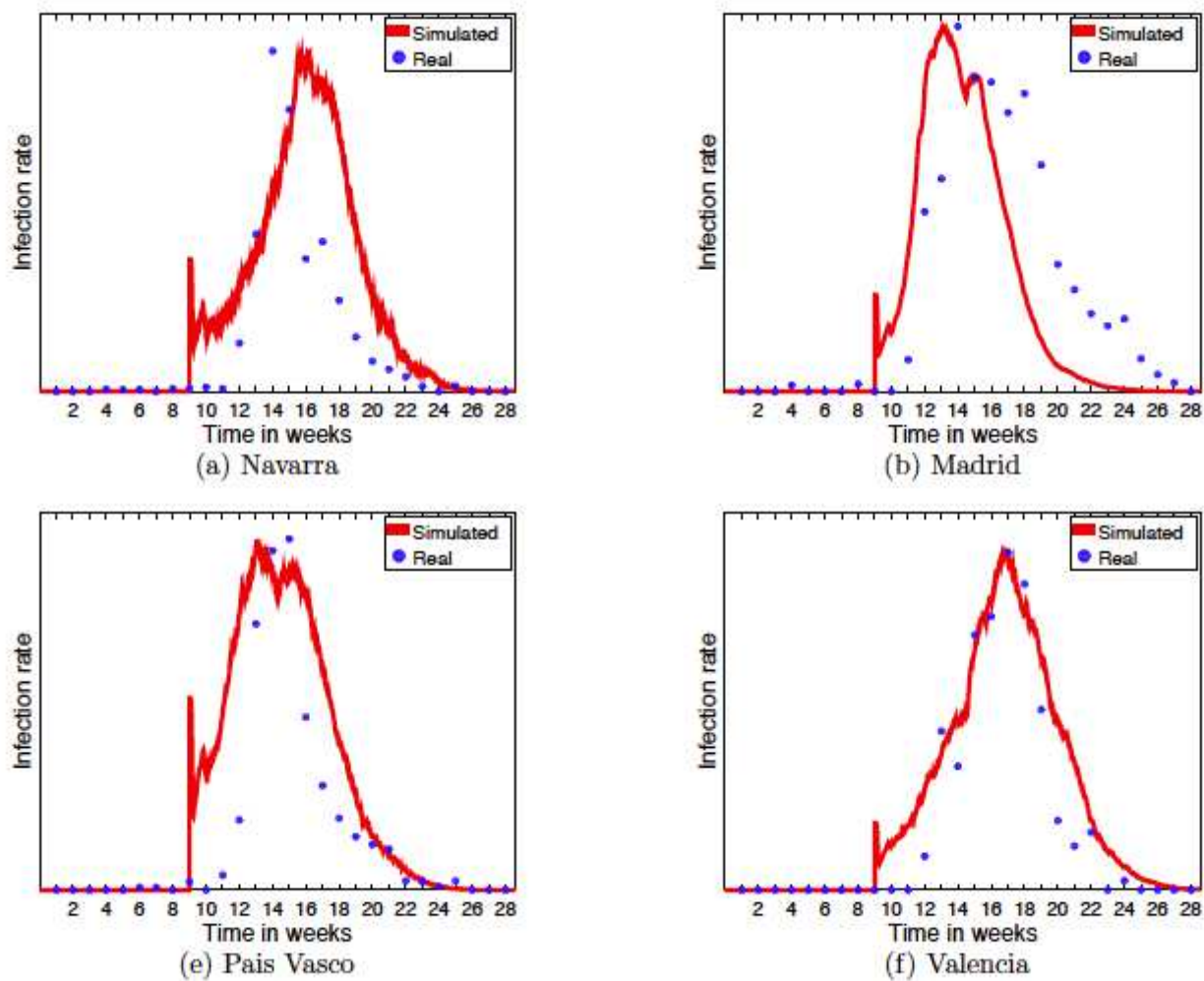


Figure 3

Comparison of normalized values between EpiGraph (in red) and real values (in blue) for Navarra, Madridm Pais Vasco and Valencia communities. Real values correspond to the total number of infected N_{tot} , obtained by means Equation 4 from in uenza surveillance data.

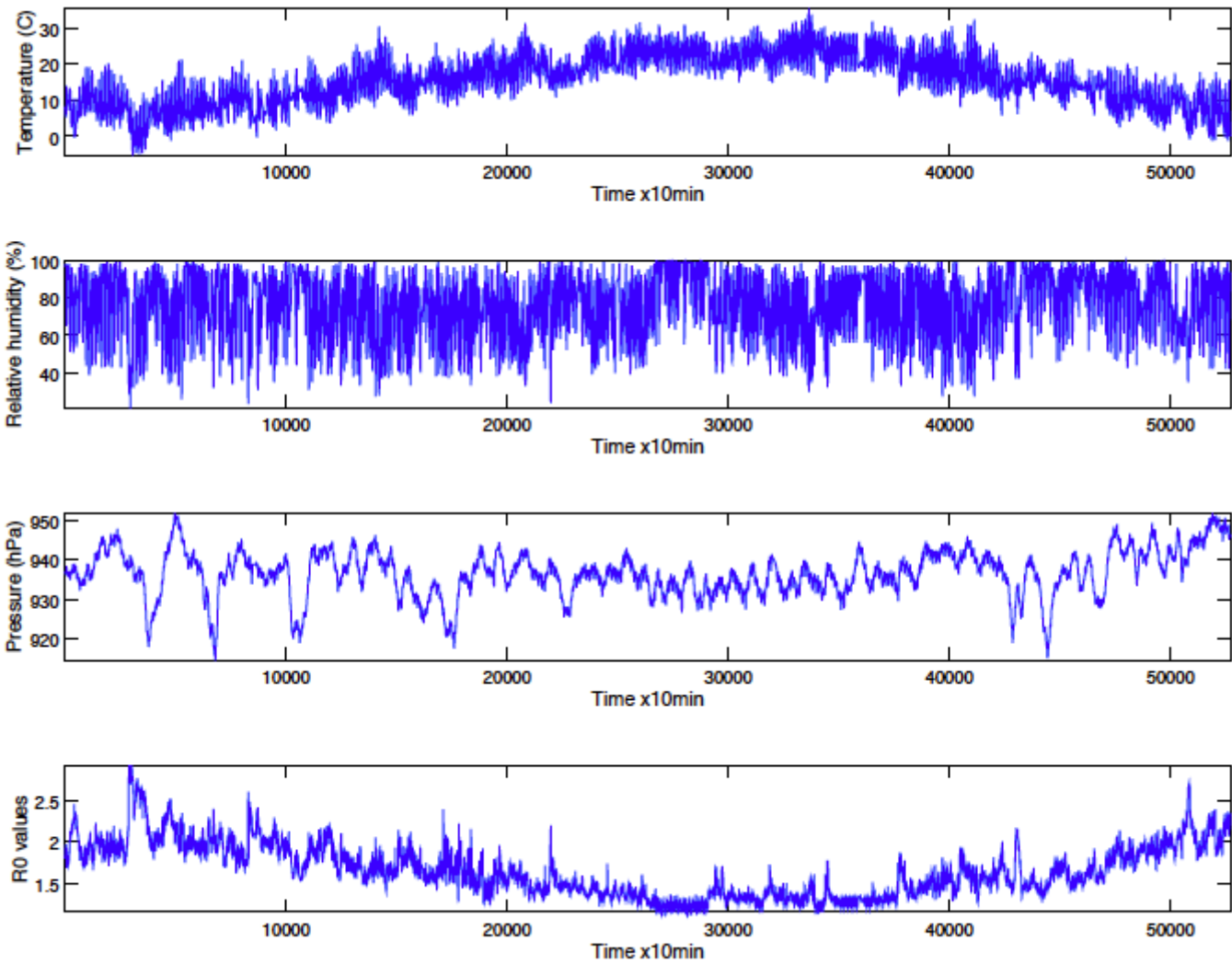


Figure 4

Meteorological parameters (T, RH, P) and the obtained R0s values for a one-year simulation (2011) for Tarrasa urban area.

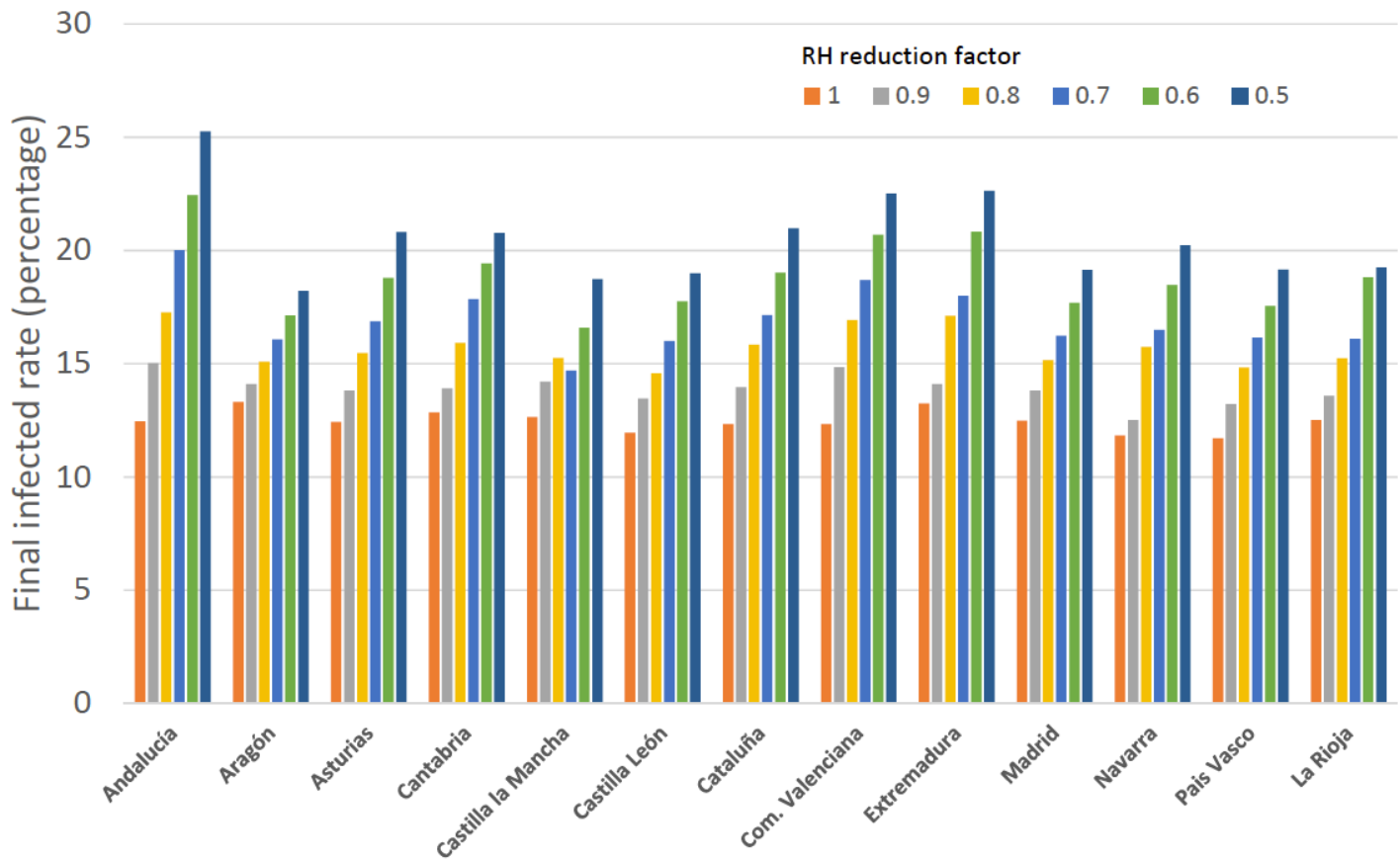


Figure 5

Effect of long-term changes of relative humidity on the influenza propagation for the different communities considered in the simulation. Meteorological parameters (T, RH, P) and the obtained R0s values for a one-year simulation (2011) for Tarrasa urban area.

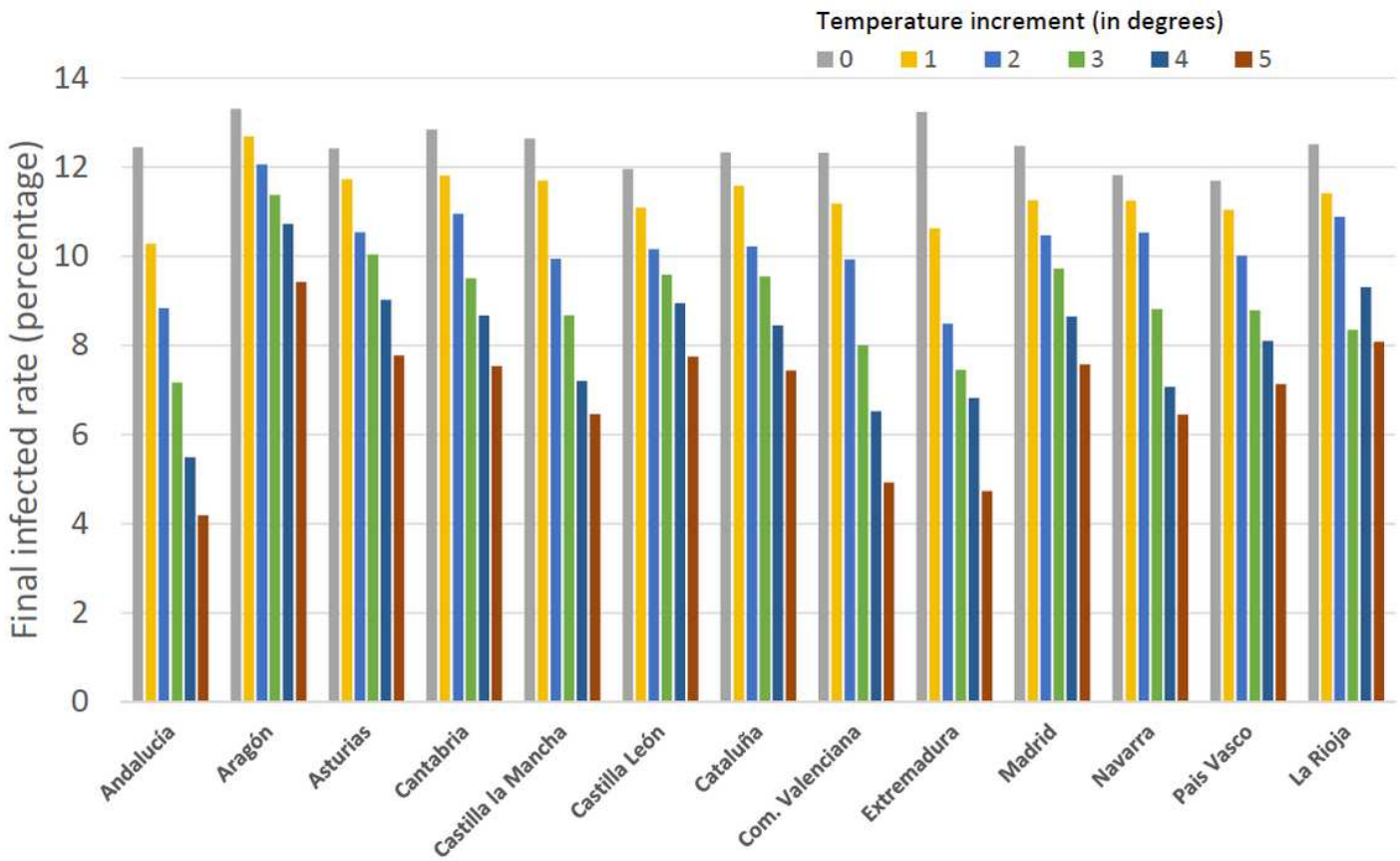


Figure 6

Effect of long-term changes in the temperature on the influenza propagation for the different communities considered in the simulation.

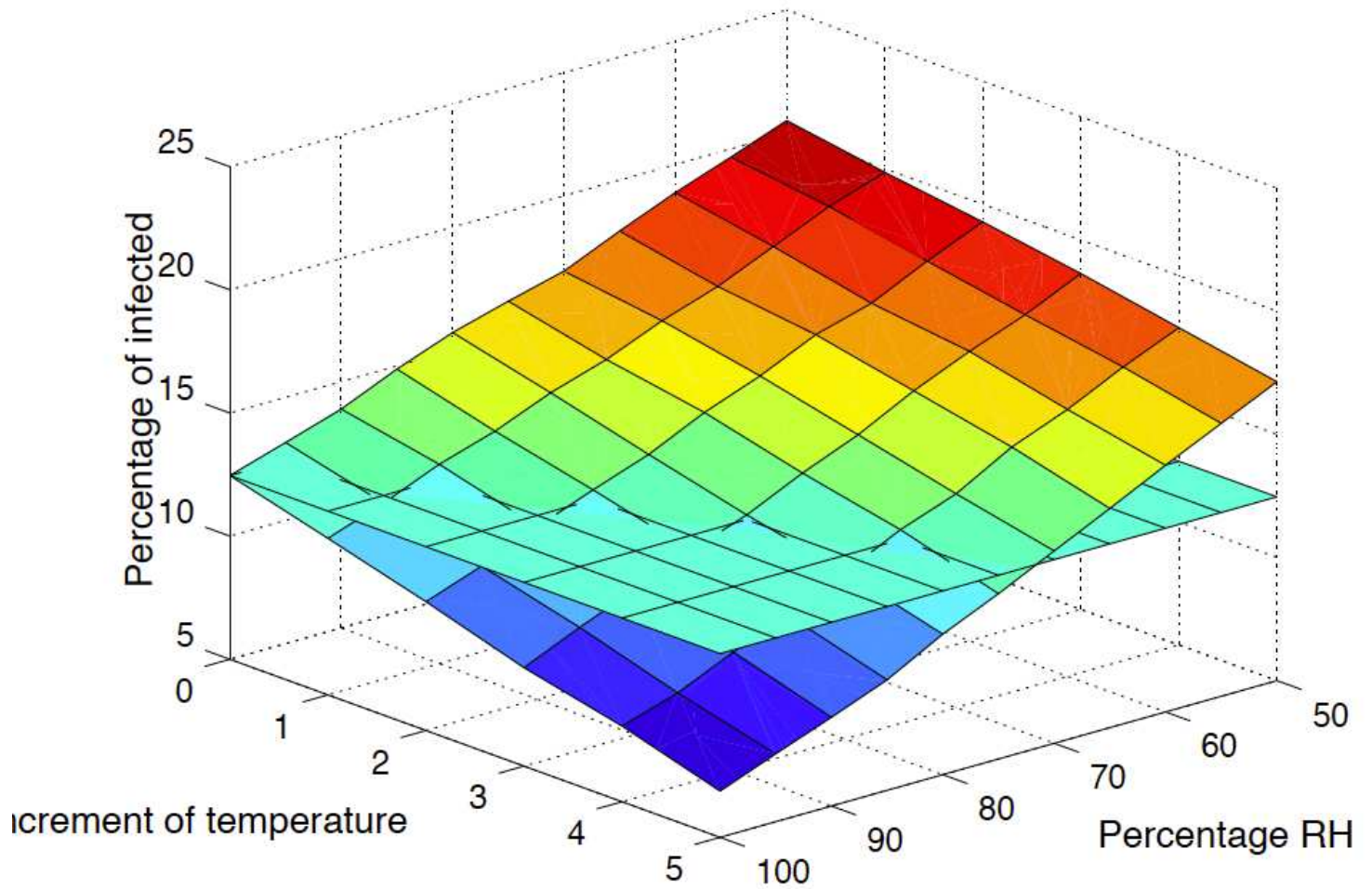
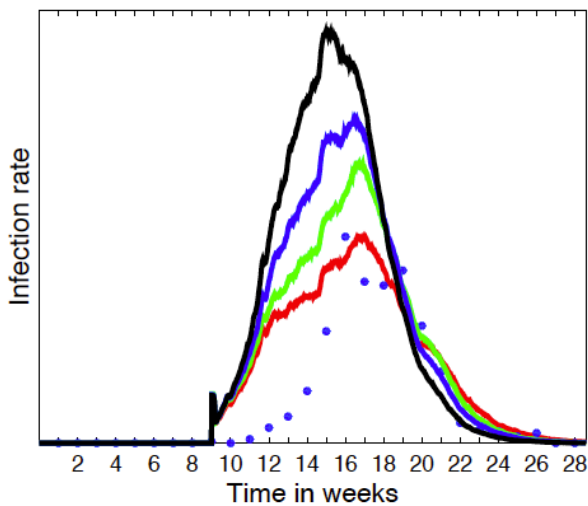
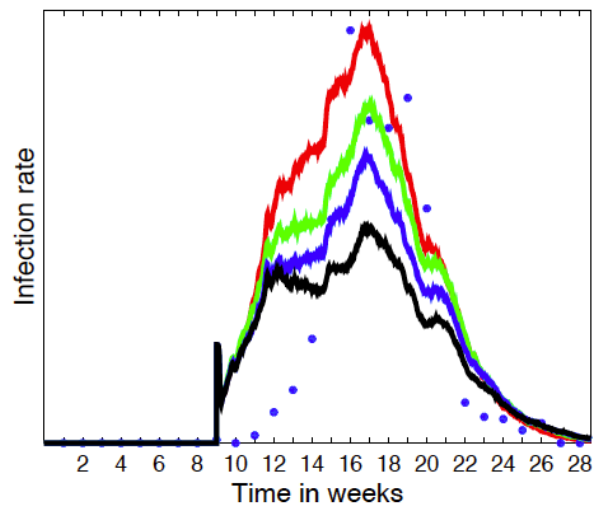


Figure 7

Effect of long-term changes in the relative humidity (percentil reduction) and temperature (value increment in Celsius) on the in uenza propagation for the average nation-wide infection rates.



(a) Effect of different RH values



(b) Effect of different T values

Figure 8

Effect of long-term parameter variation on the infection distribution shape for Andalucía. In (a) different RH scales are evaluated (100% in red, 90% in green, 80% in blue and 70% in black); In (b) different temperature offsets are evaluated (0 degrees in red, +1 degrees in green, +2 degrees in blue and +3 degrees in black).

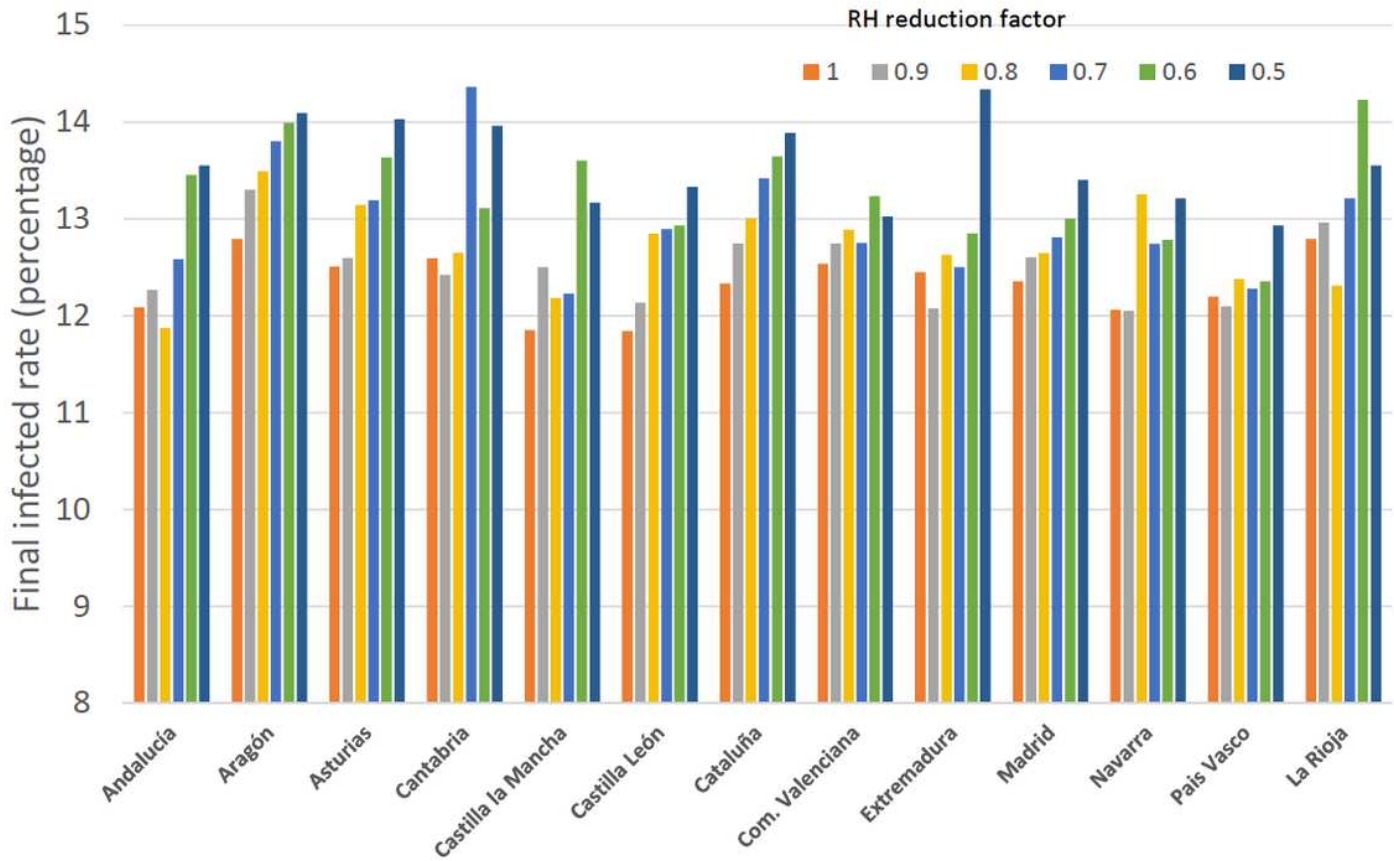


Figure 9

Effect of short-term changes in the relative humidity on the influenza propagation for the different communities considered in the simulation.

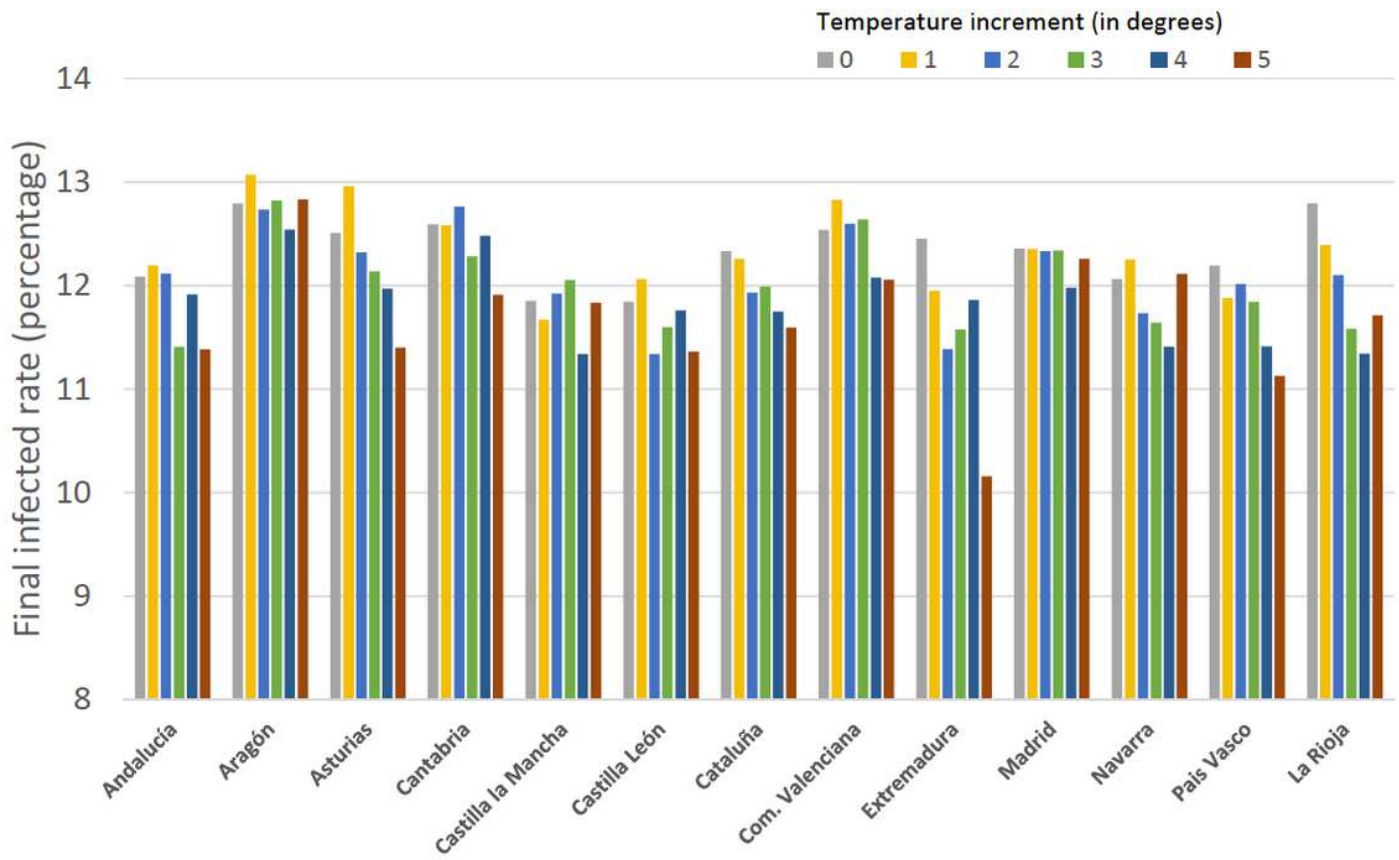


Figure 10

Effect of short-term changes in the temperature on the influenza propagation for the different communities considered in the simulation.